

Published in final edited form as:

J Orthop Res. 2013 September ; 31(9): 1430–1437. doi:10.1002/jor.22372.

Mechanical, Compositional, and Structural Properties of the Mouse Patellar Tendon with Changes in Biglycan Gene Expression

LeAnn M. Dourte¹, Lydia Pathmanathan¹, Michael J. Mienaltowski², Abbas F. Jawad³, David E. Birk², and Louis J. Soslowsky¹

¹McKay Orthopaedic Research Laboratory, University of Pennsylvania, 424 Stemmler Hall 36th Street and Hamilton Walk, Philadelphia, Pennsylvania, 19104-6081

²Department of Molecular Pharmacology and Physiology, University of South Florida Morsani College of Medicine, Tampa, Florida

³Department of Pediatrics – Biostatistics and Epidemiology, University of Pennsylvania Perelman School of Medicine/Children's Hospital of Philadelphia, Philadelphia, Pennsylvania

Abstract

Tendons have complex mechanical properties that depend on their structure and composition. Some studies have assessed the role of small leucine-rich proteoglycans (SLRPs) in the mechanical response of tendon, but the relationships between sophisticated mechanics, assembly of collagen and SLRPs have not been well characterized. In this study, biglycan gene expression was varied in a dose dependent manner using biglycan null, biglycan heterozygote and wild type mice. Measures of mechanical (tension and compression), compositional and structural changes of the mouse patellar tendon were evaluated. Viscoelastic, tensile dynamic modulus was found to be increased in the biglycan heterozygous and biglycan null tendons compared to wild type. Gene expression analyses revealed biglycan gene expression was closely associated in a dose-dependent allelic manner. No differences were seen between genotypes in elastic or compressive properties or quantitative measures of collagen structure. These results suggest that biglycan, a member of the SLRP family, plays a role in tendon viscoelasticity that cannot be completely explained by its role in collagen fibrillogenesis.

Keywords

proteoglycans; structure–function; biglycan knockout; tendon mechanics

Tendons are hierarchical tissues composed of organized collagens, proteoglycans, glycoproteins, water and cells with the extracellular matrix (ECM) components providing structural integrity to the tissue. Tendon injuries are of concern because they heal slowly and rarely regain normal function. Despite advances in surgical and therapeutic tendon repair regimens, adhesion formation, re-ruptures and decreased function are still common problems.^{1,2} Many studies have demonstrated that the composition and structure of tendon are important in the proper mechanical function of the tissue and changes in its makeup result in altered mechanics both in injury and in functional adaptation.^{3–5} Understanding

these complex tissue responses requires knowledge of how individual tendon constituents and their structural arrangement affect mechanical properties.

The predominant tensile bearing structure in tendon is collagen fibers. Many studies have focused on the role of these fibers on the tensile properties of tendon; however, fibers alone cannot completely explain the viscoelastic and nonlinear response of tendon.⁶⁻⁸ The interactions of small leucine-rich proteoglycans (SLRPs) with other ECM molecules, such as collagen fibrils, as well as their association with water are strongly indicative of the role that SLRPs may play in tendon mechanics. Specifically, class I SLRPs have been shown to have varying expression and accumulation during the development and healing processes during which large changes in mechanical properties occur.^{9,10}

Biglycan is a class I SLRP, and is involved in the regulation of collagen fibrillogenesis. Tail and quadriceps tendons from mice deficient in biglycan have tendon fibril diameters that are decreased compared to wild type while the distribution of the fibril sizes is age and tendon specific.^{4,11} Mechanical properties are also altered in a tendon specific manner¹² and may be due to the correlation previously noted between collagen fibril diameter and/or area fraction and elastic tensile properties.¹²⁻¹⁴ In addition to complications associated with variation with age and tendon type, it is often difficult to draw relationships between collagen structure, tendon mechanics, and biglycan content since it is unknown if the mechanical changes were a result of collagen changes or the inherent effect of the reduction of biglycan. A more comprehensive understanding of these relationships, particularly in the areas of nonlinear, viscoelastic and compressive mechanics where biglycan may play a large role, is therefore needed.

The objective of this study was to evaluate the structural, compositional and mechanical changes related to differences in biglycan gene expression. A dose response was created by using biglycan null ($Bgn^{-/-}$), heterozygote ($Bgn^{+/-}$) and wild type (WT, $Bgn^{+/+}$) mouse patellar tendons. We hypothesized that in the $Bgn^{-/-}$ mice compared to WT, tensile elastic, tensile viscoelastic and compressive elastic properties would be decreased. In the $Bgn^{+/-}$, tensile viscoelastic and compressive properties also would be decreased, but to a lesser extent than the null mice. In both null and heterozygote mice, fibril diameters would be decreased with a larger spread. Finally, no changes would be seen in total collagen content.

Methods

Female, C57Bl/6 mice were used in this study approved by the University of Pennsylvania and University of South Florida IACUCs. All mice were sacrificed at 5 months of age to ensure skeletal maturity.³ Three different genotypes were used and included wild type mice with two functional Bgn alleles (WT, $n = 34$), biglycan heterozygotes ($Bgn^{+/-}$, $n = 36$), and biglycan null ($Bgn^{-/-}$, $n = 28$) mice.⁵ Biglycan null and heterozygous mice had a targeted disruption of the biglycan gene leading to an absence or single allele expression of this SLRP. Female mice were utilized since biglycan is X-linked and therefore females are needed to create the levels of both one and two active alleles. WT mice were obtained from Jackson Laboratories (Bar Harbor, ME). $Bgn^{-/-}$ and $Bgn^{+/-}$ mice were bred in house using approved protocols. Whenever possible, mechanical, structural and compositional assays were performed in the same mouse. From each mouse, one whole tendon was used for either tensile or compressive mechanics. The paired, contralateral tendon was bisected and randomly assigned to two of the three compositional or structural assays.

Tensile Mechanics

Patellar tendons were randomly removed from either the left or right limb for tensile biomechanical analysis (WT $n = 14$; $Bgn^{+/-}$ $n = 14$; $Bgn^{-/-}$ $n = 15$). and carefully dissected

under a microscope leaving the patella–tendon–tibia complex intact. The cross-sectional area was measured using a laser based system. The tibia was potted in polymethylmethacrylate (PMMA) and the tendon was coated uniformly with small speckles of Verhoeff stain using a fine bristled brush for local optical strain analysis. The potted tibia was gripped and the patella held in a custom fixture. Specimens were submerged in a 37°C PBS bath and tensile tested.

Specimens were preloaded, preconditioned and allowed to recover before viscoelastic testing. Three levels of stress relaxation were performed (4%, 6%, and 8% strain), each followed by a frequency sweep at an amplitude of 0.125% calculated from grip-to-grip strain.¹⁵ Following viscoelastic testing, a ramp to failure was performed with optical strain analysis. Data was converted to the frequency domain and dynamic modulus (ratio of the magnitude of the stress over the strain) and phase angle were calculated. A bilinear fit was applied to the ramp to failure to obtain the elastic properties toe and linear stiffness, toe and linear modulus and the transitional displacement or strain defined by the breakpoint in the bilinear fit. Percent relaxation was calculated at each strain level. Tendon length at preload also was calculated from the optical analysis.

Compressive Mechanics

For compressive testing, patellar tendons were randomly removed from either the left or right limb (WT $n = 13$; $Bgn^{+/-} n = 13$; $Bgn^{-/-} n = 12$) and dissected under a microscope leaving the patella–tendon–tibia complex intact. Specimens were attached to a testing stage using cyanoacrylate¹⁶ and flooded with PBS. A 26SW gauge steel wire was used to create a custom, flat ended, cylindrical indenter with a diameter of 0.018 in. (0.4572 mm). A tare load of -0.002 N was applied and the thickness of the tendon was defined from that point to the testing stage. Six incremental indents of 4% strain at 0.3%/s were applied with 1,200 s of relaxation between each step. A Poisson's ratio of $\nu_{loading} = 0.5$ was assumed for the loading portion of the curves¹⁷ and the Hayes model¹⁶ with finite deformation¹⁸ was used to calculate shear modulus, Poisson's ratio of the solid matrix, peak modulus, and equilibrium modulus. Data from the third indentation corresponding to 12% strain were used for analysis.

Total Collagen Content

For analysis of total collagen content, tendons were dried at 65°C for 24 h and weights obtained. The tissue was digested in 5 mg/ml proteinase K solution at 65°C for 18 h. Acid hydrolysis was completed in sealed glass vials with 6 N HCL and heated to 110°C for 16 h. Samples were subsequently neutralized by evaporating off HCl in a lyophilizer with NaOH and resuspended in water. *o*-Hydroxy-proline (OHP), a measure of collagen content, was determined colorimetrically by reaction of the digest with *p*-benzaminoaldehyde and chloramine-T. OHP content was converted to total collagen content using a 1:14 ratio of OHP to collagen and normalized by dry weight.¹⁹

Gene Expression

As a means of examining biglycan gene expression, assuming transcript abundance is representative of protein levels, mRNA expression levels were determined for biglycan via real-time quantitative polymerase chain reaction assay (qPCR). Immediately following dissection and bisection, tendon samples were flash frozen in liquid nitrogen and stored at -80°C until analysis. Individual samples were treated as previously described with 5 ng of SPIA cDNA being used per qPCR reaction.²¹ Mouse specific primers for beta-actin (Act—F: AGATGACCCAGATCATGTTTGAGA; R: CACAGCCTGGATGGCTACGT), and biglycan (Bgn—F: CCTTCCGCTGCGTACTGA; R: GCAACCACTGCCTCTA-CTTCTTATAA) were used. Each patellar tendon sample was analyzed in triplicate. Gene

specific efficiencies were calculated²² for each qPCR plate and the relative quantity of mRNA for each gene of interest was computed using the comparative efficiency($-C_t$) method (ABI Sequence Detection System User Bulletin 2) relative to Act-. Expressional analyses (Supplementary Methods) of pooled WT and *Bgn*^{-/-} patellar tendons were also performed to investigate possible compensation of other proteoglycans (decorin, fibromodulin, lumican).

Transmission Electron Microscopy

Collagen fibril structure in the patellar tendon was analyzed using transmission electron microscopy (TEM). Tendons were fixed in situ and processed as previously described.²³ Cross-sections of tendons were examined using a JEOL 1400 transmission electron microscope (JEOL Ltd, Tokyo, Japan) equipped with an Orius widefield sidemount CCD camera (Gatan Inc., Pleasanton, CA). Micrographs were taken in the midsubstance, away from the region that may have been cut during tissue splitting. For analyses, five to six images per tendon were taken at 60,000 \times from non-overlapping regions of the central portion of the tendon. Fibril diameters were measured using a custom program (MATLAB) and were determined along the minor axis of the fibril profile. For each tendon, the quantitative parameters of mean fibril diameter and fibril diameter distribution (coefficient of variation) were averaged across all regions of interest and histograms of fibril size were created.

Statistical Analysis

For cross-sectional area, tendon length, linear and toe moduli and stiffness, ramp to failure transition points, total collagen, gene relative expression, and TEM structural parameters, a one-way ANOVA across genotype with Bonferroni post-hoc tests was performed. A two-way ANOVA across genotype and repeated strain level was used to analyze the parameter of percent relaxation with Bonferroni post-hoc tests. For viscoelastic parameters in the frequency sweep, a three-way ANOVA comparing the effects of genotype, strain level and repeated frequencies was performed. For significant interaction terms, simple effects were analyzed using a Bonferroni post-hoc analysis. Significance for all ANOVAs was set at $p < 0.05$. Significance for post-hoc tests using Bonferroni corrections was set at $p < 0.05/n$ corrected by the number of comparisons, n , and is therefore evaluated as $p < 0.05/n$.

Results

Patellar tendons from all three genotypes appeared normal and ectopic ossification was not observed grossly in any of the tendons. Cross-sectional area was significantly decreased in the *Bgn*^{+/-} mice compared to wild type and *Bgn*^{-/-} (WT 0.25 ± 0.03 mm², *Bgn*^{+/-} 0.21 ± 0.05 mm², *Bgn*^{-/-} 0.26 ± 0.05 mm², mean \pm SD, $p < 0.05/3$ vs. *Bgn*^{+/-}). Tendon length at preload was found to be significantly greater in the *Bgn*^{-/-} than both WT and *Bgn*^{+/-} (WT 3.19 ± 0.26 mm, *Bgn*^{+/-} 3.07 ± 0.34 mm, *Bgn*^{-/-} 3.49 ± 0.27 mm, mean \pm SD, $p < 0.05/3$ vs. *Bgn*^{-/-}).

Tensile Mechanics

Contrary to our hypothesis, no differences between genotypes were seen in any tensile elastic parameter including toe region stiffness and modulus, linear region stiffness and modulus, or transition displacement and strain (Table 1). In the viscoelastic property percent relaxation, no differences were seen between genotypes but percent relaxation significantly decreased with increasing strain level (Fig. 1). Specifically, all strain levels were significantly different from each other (4% vs. 6%, 4% vs. 8%, 6% vs. 8%).

Dynamic modulus was significantly affected by genotype (Fig. 2). There was an interaction between frequency and genotype with Bonferroni post hoc tests for simple effects showing that both *Bgn*^{+/-} and *Bgn*^{-/-} had a significantly higher dynamic modulus than wild type at all frequency levels. Dynamic modulus also significantly increased with both increasing strain level and frequency with an interaction between the two. At a specific frequency, all strain levels were different from each other (Fig. 3A). Also, at each strain level, all frequencies were significantly different from each other except 0.01 Hz versus 0.1 Hz at all frequencies, 1 Hz versus 10 Hz at 4%, and 5 Hz versus 10 Hz at 8% (Fig. 3B). This frequency dependence can be difficult to see due to sample variance but due to the design of the study, repeated measures ANOVA testing allows for analysis of the within sample variation. Therefore representative single sample *Bgn*^{-/-} plots at 4% strain are shown in which the change with frequency is clearer (Fig. 4). Both WT and *Bgn*^{+/-} samples followed similar patterns. No differences were seen between genotypes in dynamic stiffness (Table 2) or phase shift (Table 3).

Compressive Mechanics

Genotype was shown to have no significant effect on any compressive property (Table 4). This included compressive shear modulus, peak modulus, equilibrium modulus, and Poisson's ratio of the solid matrix.

Total Collagen Content

The total collagen content was not significantly affected by genotype in agreement with our hypothesis (WT 837.9 ± 267.3 g/mg, *Bgn*^{+/-} 737.0 ± 297.7 g/mg, *Bgn*^{-/-} 701.7 ± 238.1 g/mg, mean ± SD).

Gene Expression

There was an allele dependent expression of *Bgn* (Fig. 5). As expected, *Bgn* gene expression in the null mice was at background. *Bgn* gene expression in heterozygous mice was approximately half that of wild type mice. In addition, there was no compensation for loss of *Bgn* by the expression of other closely related SLRPs (Supplemental Fig. S1). The expression of decorin (*Dcn*), fibromodulin (*Fmod*), and lumican (*Lum*), was comparable in wild type and *Bgn*^{-/-} patellar tendons.

Transmission Electron Microscopy

Overall, collagen fibrils were observed to have a uniformly circular cross-section (Fig. 6). The average fibril diameter was not significantly affected by genotype (WT 95.4 ± 7.1 nm, *Bgn*^{+/-} 99.1 ± 9.3 nm, *Bgn*^{-/-} 99.4 ± 8.2 nm, mean ± SD). No differences were found in fibril diameter spread (coefficient of variation; WT 0.42 ± 0.04, *Bgn*^{+/-} 0.39 ± 0.04, *Bgn*^{-/-} 0.39 ± 0.05, mean ± SD). In light of these results, histograms of the fibril size distribution have been provided (Fig. 6). Qualitatively, the histograms of fibril diameter show a small increase in larger fibrils (longer tail) in the *Bgn*^{+/-} (Fig. 6A and B). In the *Bgn*^{-/-}, the density of large fibrils appears to be increased compared to WT (Fig. 6A and C).

For additional interpretation of the results, exact *p* values can be found in Supplementary Tables 1–8.

Discussion

This study explored the biglycan dose-dependent changes in mechanical, structural and compositional properties for mature patellar tendons. By examining both collagen and SLRP changes, this study evaluated the influence on mechanics from both the physical effect of the

biglycan glycoprotein and collagen changes. By doing so, this study explored fundamental structure–function relationships in the mature patellar tendon.

Surprisingly, no significant differences were found in collagen characteristics in either the *Bgn*^{-/-} or *Bgn*^{+/-}. Qualitatively, the fibril spread in the *Bgn*^{+/-} has an increased large fibril diameter “tail” and *Bgn*^{-/-} has a small increase in aggregation of larger fibrils. Previous studies have shown the role of biglycan in collagen fibrillogenesis to be tissue specific. For example, in 2-month-old male *Bgn*^{-/0} mice, fibrils in the bone and skin had increased average diameter and spread whereas in the tail tendons, fibril average was decreased and spread increased.⁴ However, 3-month-old mouse quadriceps tendons were shown to have decreased average diameters and decreased spread.¹¹ These results suggest that the role of biglycan in collagen fibrillogenesis are also tendon, and possibly age, specific and may explain some of the tendon specific changes in mechanics.

Biglycan gene expression was allelic dose-dependent. *Bgn* gene expression was greatest in wild type tendons, significantly decreased in *Bgn*^{+/-} tendons to approximately half that seen in WT tendons and, as expected, the *Bgn* expression was absent in *Bgn*^{-/-} tendons. However, besides having increasing trends for expressional differences, compensation from other proteoglycans *Dcn*, *Fmod*, and *Lum* was not detected. Thus, differences seen in mechanical parameters among the three genotype groups are most closely associated with number of functional *Bgn* alleles.

No changes were seen in any elastic property. This result is in agreement with a previous study in 8- to 10-week old *Bgn*^{-/-} mouse patellar tendons and tail tendon fascicles.¹² However, in the same animals, *Bgn*^{-/-} FDL tendons had increased linear region modulus. These results suggest that in vivo loading environment, and therefore tendon type, is an important factor in determining structure function relationships. In addition, the hierarchical level of collagen being analyzed may also play a role and future studies may lend further insight into possible relationships.

In tendon viscoelastic properties, dynamic modulus was significantly increased from wild type at all frequencies in the *Bgn*^{+/-}. Dynamic modulus may better represent the small displacement, cyclic loading a tendon undergoes on a daily basis. The only other measured differences between wild type and *Bgn*^{+/-} were decreased biglycan expression and a qualitative observation of an increase in larger fibrils. This suggests that in the *Bgn*^{+/-} mice, the increased dynamic modulus may be a function of decreased biglycan and/or larger fibrils, however, the shift in collagen fibril size is minimal and was not reflected as an increase in elastic parameters as might be expected from larger fibrils.²⁴ Dynamic modulus was also significantly increased in the *Bgn*^{-/-} mice at all frequencies. In the *Bgn*^{-/-}, a small qualitative aggregation in larger fibrils was observed but was not reflected in the mean fibril diameter. Overall, alterations in the viscoelastic properties cannot be explained by changes in collagen fibril structure and are most likely attributed to decreased biglycan. These results support the hypothesis that SLRPs are responsible for maintaining spacing between collagen fibrils and that removal of them allows fibrils to interact more, increasing fibril–fibril friction and adhesions, especially under small oscillatory loading.²⁵ Additional studies are needed to further explore fibril–fibril interactions.

Phenotypic differences in cross-sectional area and tendon length could be explained by developmental disparities by genotype. Along these lines, the increase in the dynamic modulus of the *Bgn*^{+/-} but no change in dynamic stiffness compared to wild type may be explained by the decreased cross-sectional area of the *Bgn*^{+/-}. On the other hand, the increase in dynamic modulus of the *Bgn*^{-/-} with no change in dynamic stiffness is most likely due to an increased tendon length in the *Bgn*^{-/-}. While these developmental

differences aid in interpreting the results within a particular genotype, they cannot completely explain the increased dynamic modulus between genotypes since the calculation of a modulus normalizes the stiffness with respect to structure (cross-sectional area and length). This again suggests that the increases in dynamic modulus are a result of the increased population of large fibrils or decrease in biglycan.

The dynamic mechanics results in this study are in contrast to previous studies exploring similar structure–function relationships in human ligament and rat tail tendon fascicle.^{15,26} These previous studies removed the GAG chains through a digestion process, leaving the proteoglycan core behind in the interfibrillar space. The current study aimed to remove the entire biglycan proteoglycan by removing or reducing gene expression. In addition, the rat tail tendon fascicle is a hierarchical level below a structurally complete tendon which may lead to differences in how the levels interact.

The reason for the similar results between *Bgn*^{+/-} and *Bgn*^{-/-} is not immediately clear. Previous studies have suggested a possible tissue swelling effect from PBS incubation that is decreased by GAG removal.^{27,28} This phenomenon may have affected any dose dependent differences in the *Bgn*^{+/-} and *Bgn*^{-/-}. All tissues in this study were handled in a similar manner, however, results on the role of incubation and environmental salts are still unclear.^{29,30} Unfortunately, due to the small size of the bisected tendons, water content was not measured in this study. Future studies measuring water content and fixed charge density may lend additional insight into these results. Additionally, previous studies have shown regional property changes with GAG digestion.³¹ Future studies exploring regional differences may explain the similar results in *Bgn*^{+/-} and *Bgn*^{-/-} tendons.

In both *Bgn*^{-/-} and *Bgn*^{+/-} no differences were found in any compressive property, despite significant reductions in biglycan suggesting that biglycan does not play a role in the instantaneous or equilibrium compressive properties of the patellar tendon. While unconfined compression was chosen to better represent the natural boundary conditions of the tendon, future testing with other models may yield useful data on the role of PGs/GAGs in controlling the time-dependent fluid flow both through the tissue and parallel to the collagen fibers.³²

In this study, the patellar tendon was chosen for its relatively simple in vivo loading environment, without applied compression or shear from other structures that can result in the altered gene expression and disorganized collagen fibrils often seen in other tendons. This leads us to hypothesize that the relationships found between structure/composition and mechanics found in this study will hold true for other tendons. The change in fibril characteristics with decreases in biglycan expression previously found in other tendons^{4,11} may be a result of their loading environment or age. Thus, if similar relationships between structure/composition and mechanics do not exist, then it could be due to anatomical location-specific considerations.

As with any study, there are several limitations that must be considered when interpreting our results. Due to the X-linked nature of the biglycan gene, only female mice were used in this study which may lead to unaccounted variation between samples. Additionally, while the aim of this study was to characterize properties at a discrete instant in time, compensatory effects that would be present throughout development in the mutant mice might still have an unmeasured effect on the data. Therefore, all changes measured in this study are due to a combination of developmental and structure–function effects and we have tried to note this possibility where applicable. Finally, it is important to note that in this study, relative mRNA expression was measured rather than protein levels. Previous studies

have shown a relationship between biglycan gene and protein expression in C57Bl/6 wild type mouse tendon,²⁰ however, future studies are needed to confirm this in the mutant mice.

In conclusion, this study characterized the mechanical, compositional and structural properties of mature tendon at a defined age and in a specific tendon with changes in the amount of biglycan. It demonstrated that changes in collagen content and structure cannot account for the changes in tendon viscoelastic properties with decreased biglycan expression. Future studies are needed to explore the collagen fibril–fibril interactions with decreased biglycan.

Supplementary Material

Refer to Web version on PubMed Central for supplementary material.

Acknowledgments

The authors thank Sheila Adams for her assistance.

Grant sponsor: NIAMS/NIH; **Grant numbers:** R01 AR055543 and P30AR050950.

References

- Butler DL, Goldstein SA, Guilak F. Functional tissue engineering: the role of biomechanics. *J Biomech Eng.* 2000; 122:570–575. [PubMed: 11192376]
- Butler DL, Juncosa N, Dressler MR. Functional efficacy of tendon repair processes. *Annu Rev Biomed Eng.* 2004; 6:303–329. [PubMed: 15255772]
- Brodt MD, Ellis CB, Silva MJ. Growing C57Bl/6 mice increase whole bone mechanical properties by increasing geometric and material properties. *J Bone Miner Res.* 1999; 14:2159–2166. [PubMed: 10620076]
- Corsi A, Xu T, Chen XD, et al. Phenotypic effects of biglycan deficiency are linked to collagen fibril abnormalities, are synergized by decorin deficiency, and mimic Ehlers–Danlos-like changes in bone and other connective tissues. *J Bone Miner Res.* 2002; 17:1180–1189. [PubMed: 12102052]
- Xu T, Bianco P, Fisher LW, et al. Targeted disruption of the biglycan gene leads to an osteoporosis-like phenotype in mice. *Nat Genet.* 1998; 20:78–82. [PubMed: 9731537]
- Batson EL, Paramour RJ, Smith TJ, et al. Are the material properties and matrix composition of equine flexor and extensor tendons determined by their functions? *Equine Vet J.* 2003; 35:314–318. [PubMed: 12755437]
- Guerin HA, Elliott DM. The role of fiber-matrix interactions in a nonlinear fiber-reinforced strain energy model of tendon. *J Biomech Eng.* 2005; 127:345–350. [PubMed: 15971713]
- Elliott DM, Robinson PS, Gimbel JA, et al. Effect of altered matrix proteins on quasilinear viscoelastic properties in transgenic mouse tail tendons. *Ann Biomed Eng.* 2003; 31:599–605. [PubMed: 12757203]
- Woo SL, Debski RE, Zeminski J, et al. Injury and repair of ligaments and tendons. *Annu Rev Biomed Eng.* 2000; 2:83–118. [PubMed: 11701508]
- Ansorge HL, Adams S, Birk DE, et al. Mechanical, compositional, and structural properties of the post-natal mouse Achilles tendon. *Ann Biomed Eng.* 2011; 39:1904–1913. [PubMed: 21431455]
- Ameye L, Aria D, Jepsen K, et al. Abnormal collagen fibrils in tendons of biglycan/fibromodulin-deficient mice lead to gait impairment, ectopic ossification, and osteoarthritis. *FASEB J.* 2002; 16:673–680. [PubMed: 11978731]
- Robinson PS, Huang TF, Kazam E, et al. Influence of decorin and biglycan on mechanical properties of multiple tendons in knockout mice. *J Biomech Eng.* 2005; 127:181–185. [PubMed: 15868800]
- Goh KL, Holmes DF, Lu HY, et al. Ageing changes in the tensile properties of tendons: influence of collagen fibril volume fraction. *J Biomech Eng.* 2008; 130:021011. [PubMed: 18412498]

14. Dressler MR, Butler DL, Wenstrup R, et al. A potential mechanism for age-related declines in patellar tendon biomechanics. *J Orthop Res.* 2002; 20:1315–1322. [PubMed: 12472246]
15. Lujan TJ, Underwood CJ, Jacobs NT, et al. Contribution of glycosaminoglycans to viscoelastic tensile behavior of human ligament. *J Appl Physiol.* 2009; 106:423–431. [PubMed: 19074575]
16. Hayes WC, Keer LM, Herrmann G, et al. A mathematical analysis for indentation tests of articular cartilage. *J Biomech.* 1972; 5:541–551. [PubMed: 4667277]
17. Armstrong CG, Lai WM, Mow VC. An analysis of the unconfined compression of articular cartilage. *J Biomech Eng.* 1984; 106:165–173. [PubMed: 6738022]
18. Zhang M, Zheng YP, Mak AF. Estimating the effective Young's modulus of soft tissues from indentation tests—nonlinear finite element analysis of effects of friction and large deformation. *Med Eng Phys.* 1997; 19:512–517. [PubMed: 9394898]
19. Neuman RE, Logan MA. The determination of hydroxyproline. *J Biol Chem.* 1950; 184:299–306. [PubMed: 15421999]
20. Ansoorge HL, Adams S, Jawad AF, et al. Mechanical property changes during neonatal development and healing using a multiple regression model. *J Biomech.* 2012; 45:1288–1292. [PubMed: 22381737]
21. Dourte LM, Pathmanathan L, Jawad AF, et al. Influence of decorin on the mechanical, compositional, and structural properties of the mouse patellar tendon. *J Bio-mech Eng.* 2012; 134:031005.
22. Scheffe JH, Lehmann KE, Buschmann IR, et al. Quantitative real-time RT-PCR data analysis: current concepts and the novel “gene expression's CT difference” formula. *J Mol Med.* 2006; 84:901–910. [PubMed: 16972087]
23. Birk DE, Trelstad RL. Extracellular compartments in tendon morphogenesis—collagen fibril, bundle, and macroag-gregate formation. *J Cell Biol.* 1986; 103:231–240. [PubMed: 3722266]
24. Wess, T. Collagen fibrillar structure and hierarchies. In: Fratzl, P., editor. *Collagen: structure and mechanics.* 1st. New York: Springer; 2008. p. 49-80.
25. Hall, BK. *Bone.* 1st. Caldwell, NJ: Telford Press; 1990. p. 262
26. Fessel G, Snedeker JG. Evidence against proteoglycan mediated collagen fibril load transmission and dynamic viscoelasticity in tendon. *Matrix Biol.* 2009; 28:503–510. [PubMed: 19698786]
27. Screen HR, Shelton JC, Chhaya VH, et al. The influence of noncollagenous matrix components on the micro-mechanical environment of tendon fascicles. *Ann Biomed Eng.* 2005; 33:1090–1099. [PubMed: 16133917]
28. Screen HR, Chhaya VH, Greenwald SE, et al. The influence of swelling and matrix degradation on the micro-structural integrity of tendon. *Acta Biomater.* 2006; 2:505–513. [PubMed: 16839828]
29. Svensson RB, Hassenkam T, Grant CA, et al. Tensile properties of human collagen fibrils and fascicles are insensitive to environmental salts. *Biophys J.* 2010; 99:4020–4027. [PubMed: 21156145]
30. Haut TL, Haut RC. The state of tissue hydration determines the strain-rate-sensitive stiffness of human patellar tendon. *J Biomech.* 1997; 30:311–311.
31. Rigozzi S, Muller R, Snedeker JG. Local strain measurement reveals a varied regional dependence of tensile tendon mechanics on glycosaminoglycan content. *J Biomech.* 2009; 42:1547–1552. [PubMed: 19394024]
32. Henninger HB, Underwood CJ, Ateshian GA, et al. Effect of sulfated glycosaminoglycan digestion on the transverse permeability of medial collateral ligament. *J Biomech.* 2010; 43:2567–2573. [PubMed: 20627251]

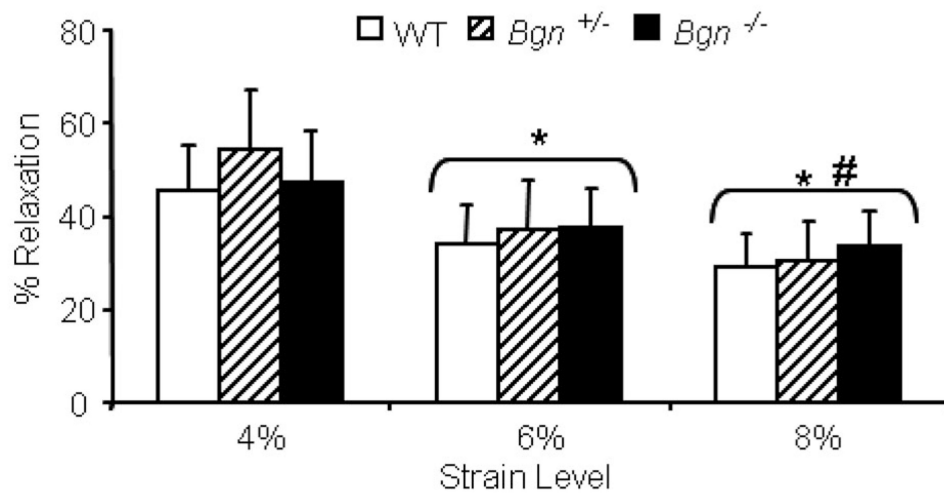


Figure 1. No differences in percent relaxation were seen between genotypes. Percent relaxation decreased with increasing strain level. Mean \pm standard deviation, $p < 0.05/3$ versus (*) 4% and (#) 6%.

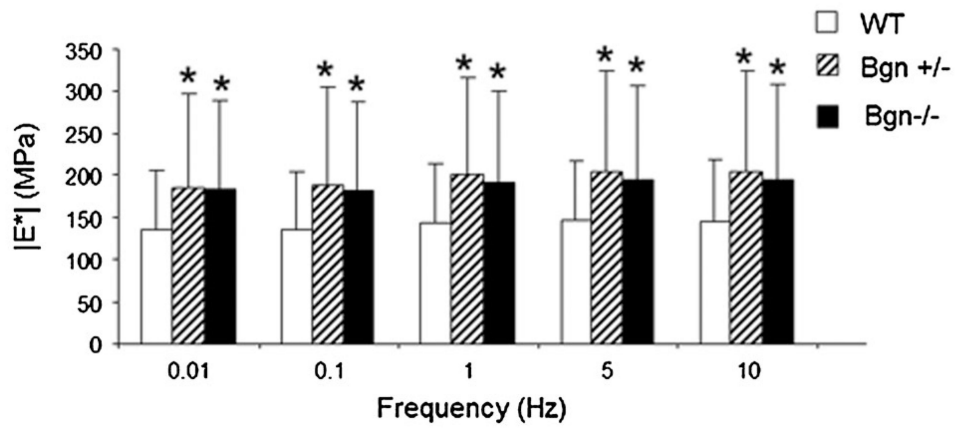


Figure 2. At every frequency level, *Bgn*^{+/-} and *Bgn*^{-/-} are significantly increased from WT. Mean ± standard deviation. Data pooled across strain level. At the given frequency, (*) *p* = 0.05/3 versus WT.

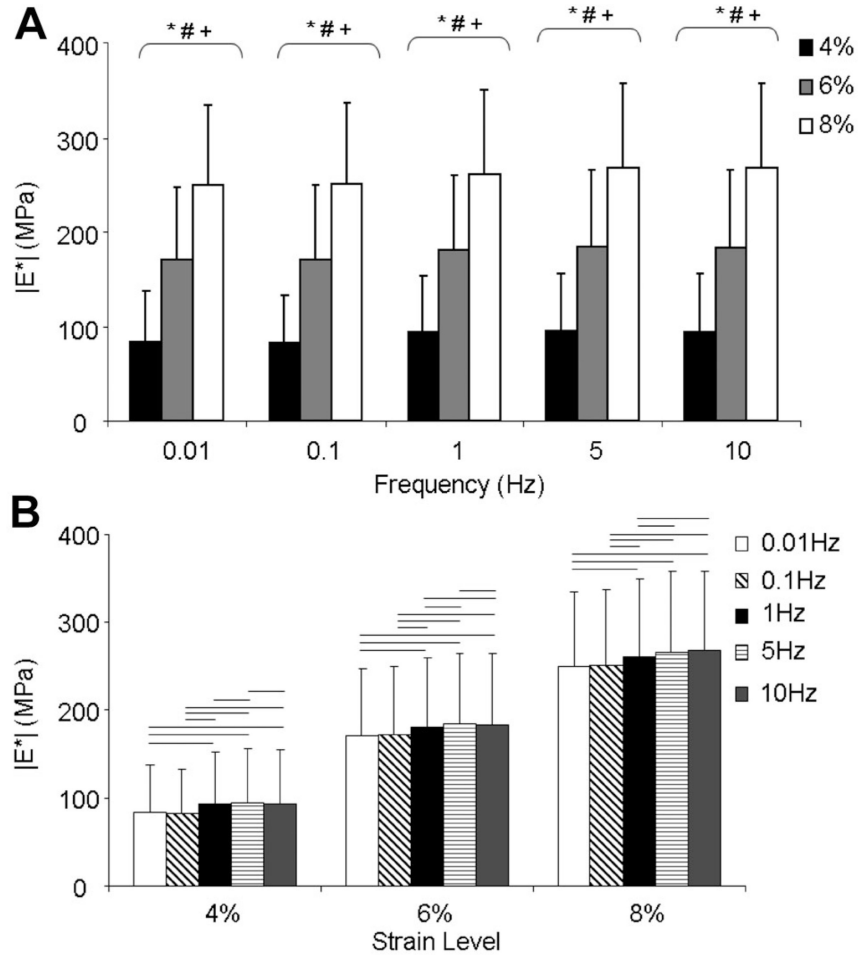


Figure 3. (A) At every frequency level, dynamic modulus significantly increased with increasing strain level. (B) At a given strain level, all combinations of frequencies were significantly different from each other (paired comparisons) except 0.01 Hz versus 0.1 Hz at 4%, 6%, and 8%, 1 Hz versus 10 Hz at 4%, and 5 Hz versus 10 Hz at 8%. Mean \pm SD. Data pooled across genotype. At the given frequency level, $p < 0.05/3$ for (*) 4% versus 6%, (#) 4% versus 8%, (+) 6% versus 8%. At the given strain level, bar denotes $p < 0.05/10$, paired comparisons.

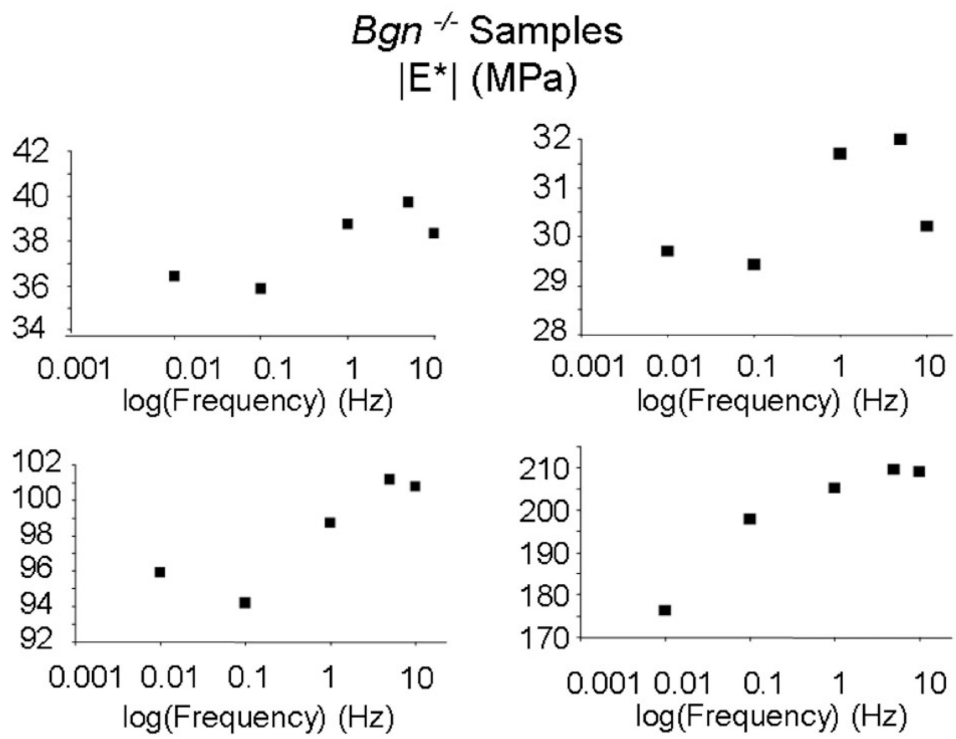


Figure 4. Dynamic modulus of representative *Bgn*^{-/-} tendons at 4% strain demonstrating frequency dependence. Similar patterns were seen in all genotypes.

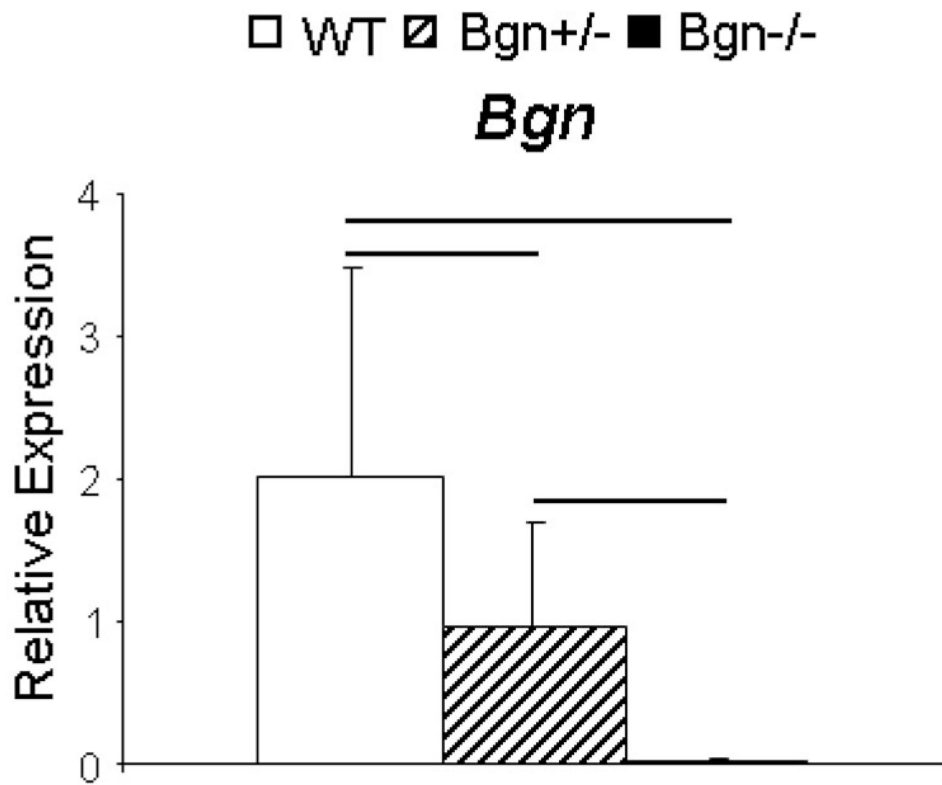


Figure 5. *Bgn* gene expression is directly related to allele number. Relative biglycan gene expression was absent in the *Bgn*^{-/-}. There was a significant decrease from WT in the *Bgn*^{+/-} tendons to approximately 50%, consistent with the absence of one allele. Mean ± SD. Bar denotes *p* 0.05/3.

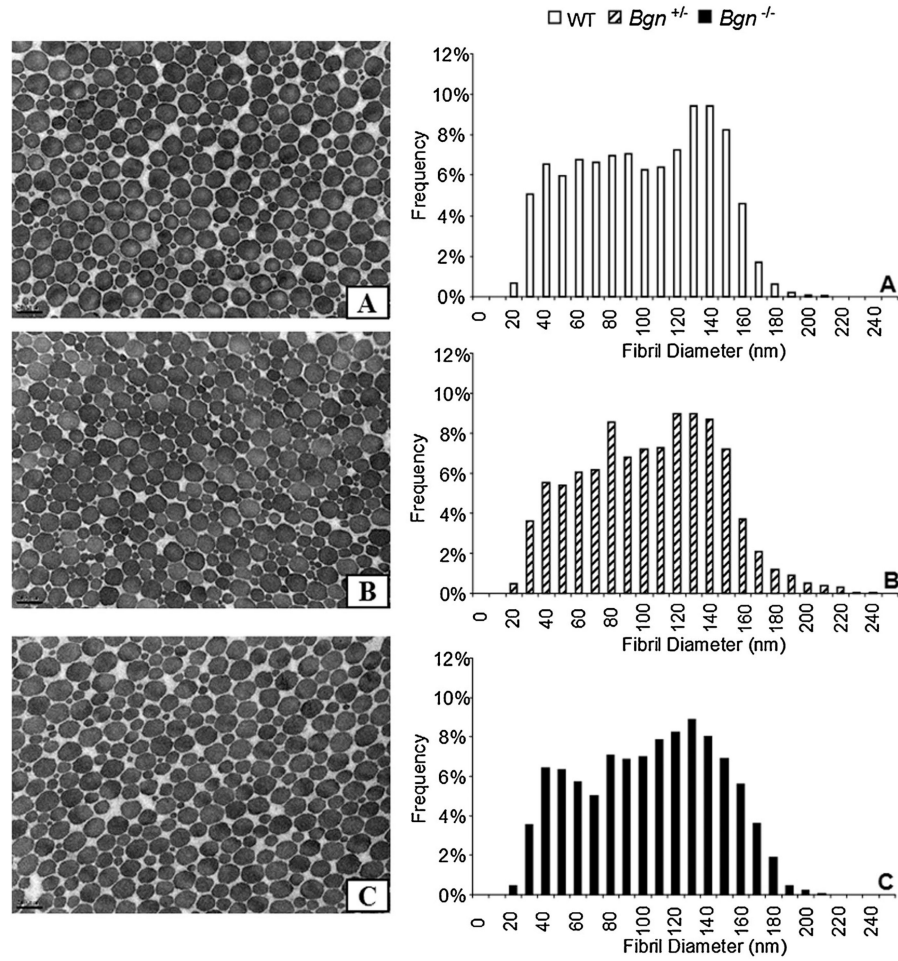


Figure 6.

Representative TEM images of fibril cross-sections and histograms of collagen fibril diameters in (A) WT, (B) *Bgn*^{+/-}, and (C) *Bgn*^{-/-} tendons. In all genotypes, most fibrils are well-formed and circular in shape. Some fibrils were slightly abnormally shaped around the perimeter but differences in the frequency of these fibrils were not noted across genotypes. Scale bar 200 nm. Qualitatively in the *Bgn*^{+/-} a small increase in larger fibrils (longer tail) can be seen. In the *Bgn*^{-/-}, the density of large fibrils appears to be increased compared to WT.

Table 1

Tensile Elastic Properties, Mean ± SD

	Toe Stiffness (N/mm)	Linear Stiffness (N/mm)	Stiffness Transition Point (mm)	Toe Modulus (MPa)	Linear Modulus (MPa)	Modulus Transition Point (Strain)
WT	0.99 ± 0.30	12.26 ± 1.96	0.19 ± 0.02	21.8 ± 16.4	377.4 ± 146.8	0.02 ± 0.01
<i>Bgn</i> ^{+/−}	1.19 ± 0.64	13.31 ± 3.42	0.19 ± 0.02	17.1 ± 12.7	292.5 ± 107.4	0.02 ± 0.01
<i>Bgn</i> ^{−/−}	1.12 ± 0.54	13.80 ± 3.68	0.20 ± 0.02	19.5 ± 12.6	358.3 ± 219.9	0.02 ± 0.01

Table 2

Dynamic Stiffness, Mean \pm SD in N/mm

	Frequency (Hz)					
	0.01	0.1	1	5	10	
4%						
WT	5.03 \pm 2.24	5.2 \pm 2.24	5.59 \pm 2.36	5.72 \pm 2.42	5.61 \pm 2.45	
<i>Bgn</i> ^{+/-}	7.02 \pm 3.93	6.58 \pm 3.16	7.07 \pm 3.30	7.26 \pm 3.39	7.15 \pm 3.42	
<i>Bgn</i> ^{-/-}	5.91 \pm 3.71	6.10 \pm 4.09	5.70 \pm 3.43	5.84 \pm 3.51	5.74 \pm 3.56	
6%						
WT	11.05 \pm 2.72	11.18 \pm 2.92	11.72 \pm 3.05	12.00 \pm 3.12	11.96 \pm 3.16	
<i>Bgn</i> ^{+/-}	13.08 \pm 5.85	13.31 \pm 5.65	14.06 \pm 5.80	14.39 \pm 5.93	14.34 \pm 5.97	
<i>Bgn</i> ^{-/-}	12.54 \pm 5.57	12.56 \pm 5.64	13.16 \pm 5.80	13.49 \pm 5.93	13.47 \pm 5.98	
8%						
WT	16.63 \pm 2.52	17.23 \pm 3.61	17.97 \pm 3.68	18.41 \pm 3.77	18.43 \pm 3.79	
<i>Bgn</i> ^{+/-}	19.05 \pm 6.06	19.73 \pm 5.87	20.52 \pm 6.06	20.97 \pm 6.19	20.97 \pm 6.23	
<i>Bgn</i> ^{-/-}	19.33 \pm 5.69	19.09 \pm 5.47	19.92 \pm 5.64	20.40 \pm 5.76	20.43 \pm 5.80	

Table 3

Phase Shift, Mean \pm SD in Degrees

	Frequency (Hz)					
	0.01	0.1	1	5	10	
4%						
WT	3.25 \pm 1.12	3.37 \pm 1.05	2.67 \pm 0.65	2.39 \pm 0.53	2.31 \pm 0.97	
<i>Bgn</i> ^{+/−}	3.94 \pm 2.03	3.94 \pm 1.36	2.82 \pm 0.89	2.35 \pm 0.73	1.97 \pm 0.83	
<i>Bgn</i> ^{−/−}	3.45 \pm 1.08	3.30 \pm 1.02	2.79 \pm 0.98	2.32 \pm 0.60	2.04 \pm 0.67	
6%						
WT	2.39 \pm 0.45	2.09 \pm 0.46	1.75 \pm 0.25	1.62 \pm 0.34	1.35 \pm 0.75	
<i>Bgn</i> ^{+/−}	2.44 \pm 1.05	2.47 \pm 0.74	1.88 \pm 0.27	1.60 \pm 0.26	1.21 \pm 0.32	
<i>Bgn</i> ^{−/−}	2.54 \pm 0.72	2.17 \pm 0.50	1.94 \pm 0.50	1.64 \pm 0.41	1.27 \pm 0.41	
8%						
WT	2.13 \pm 0.61	1.84 \pm 0.21	1.71 \pm 0.18	1.60 \pm 0.46	1.38 \pm 0.83	
<i>Bgn</i> ^{+/−}	2.51 \pm 0.75	1.89 \pm 0.27	1.62 \pm 0.14	1.33 \pm 0.14	0.91 \pm 0.17	
<i>Bgn</i> ^{−/−}	2.32 \pm 0.70	1.73 \pm 0.25	1.63 \pm 0.25	1.38 \pm 0.26	0.91 \pm 0.27	

Table 4
Compressive Properties, Mean \pm SD

	WT	<i>Bgn</i>^{+/-}	<i>Bgn</i>^{-/-}
Shear modulus (kPa)	9.6 \pm 3.2	8.7 \pm 3.7	7.8 \pm 3.4
Poisson's ratio	0.40 \pm 0.04	0.41 \pm 0.03	0.41 \pm 0.05
Peak modulus (kPa)	28.8 \pm 9.7	26.6 \pm 11.0	23.5 \pm 10.2
Equilibrium modulus (kPa)	25.9 \pm 8.1	24.7 \pm 10.2	21.8 \pm 9.6